



RESEARCH LETTER

10.1002/2017GL076520

Key Points:

- Increased carbon dioxide consistently drives reduced eastern and central Amazonian precipitation in global climate models
- Projected Amazonian precipitation changes are dominated by the carbon dioxide physiological effect
- Highlights importance of reducing uncertainties associated with vegetation schemes

Supporting Information:

- Supporting Information S1

Correspondence to:

T. B. Richardson,
t.b.richardson@leeds.ac.uk

Citation:

Richardson, T. B., Forster, P. M., Andrews, T., Boucher, O., Faluvegi, G., Fläschner, D., et al. (2018). Carbon dioxide physiological forcing dominates projected eastern Amazonian drying. *Geophysical Research Letters*, 45, 2815–2825. <https://doi.org/10.1002/2017GL076520>

Received 23 NOV 2017

Accepted 3 MAR 2018

Accepted article online 12 MAR 2018

Published online 26 MAR 2018

Carbon Dioxide Physiological Forcing Dominates Projected Eastern Amazonian Drying

T. B. Richardson¹ , P. M. Forster¹ , T. Andrews² , O. Boucher³ , G. Faluvegi⁴ , D. Fläschner⁵, M. Kasoar⁶ , A. Kirkevåg⁷ , J.-F. Lamarque⁸ , G. Myhre⁹ , D. Olivé⁷, B. H. Samset⁹ , D. Shawki⁶ , D. Shindell¹⁰ , T. Takemura¹¹ , and A. Voulgarakis⁶

¹School of Earth and Environment, University of Leeds, Leeds, UK, ²Met Office Hadley Centre, Exeter, UK, ³Institut Pierre-Simon Laplace, Université Pierre et Marie Curie/CNRS, Paris, France, ⁴NASA Goddard Institute for Space Studies and Center for Climate Systems Research, Columbia University, New York, NY, USA, ⁵Max-Planck-Institut für Meteorologie, Hamburg, Germany, ⁶Imperial College London, London, UK, ⁷Norwegian Meteorological Institute, Oslo, Norway, ⁸NCAR/UCAR, Boulder, CO, USA, ⁹CICERO Center for International Climate and Environmental Research, Oslo, Norway, ¹⁰Nicholas School of the Environment, Duke University, Durham, NC, USA, ¹¹Research Institute for Applied Mechanics, Kyushu University, Fukuoka, Japan

Abstract Future projections of east Amazonian precipitation indicate drying, but they are uncertain and poorly understood. In this study we analyze the Amazonian precipitation response to individual atmospheric forcings using a number of global climate models. Black carbon is found to drive reduced precipitation over the Amazon due to temperature-driven circulation changes, but the magnitude is uncertain. CO₂ drives reductions in precipitation concentrated in the east, mainly due to a robustly negative, but highly variable in magnitude, fast response. We find that the physiological effect of CO₂ on plant stomata is the dominant driver of the fast response due to reduced latent heating and also contributes to the large model spread. Using a simple model, we show that CO₂ physiological effects dominate future multimodel mean precipitation projections over the Amazon. However, in individual models temperature-driven changes can be large, but due to little agreement, they largely cancel out in the model mean.

Plain Language Summary Climate models show that rainfall in the eastern Amazon may decrease during the 21st century; however, the changes are uncertain and there are many factors which could affect rainfall in the region. In this study we use a range of global climate model experiments to investigate how Amazonian rainfall responds to different drivers, such as carbon dioxide in the atmosphere. We find that increasing carbon dioxide reduces east Amazonian rainfall, and this is due to the response of plant stomata to carbon dioxide. Plant stomata do not open as wide when carbon dioxide is increased, which is known as the physiological effect. The physiological effect reduces evaporation from plants which means that there is less moisture available to fuel rainfall. We construct a simple model to estimate future rainfall changes over the Amazon to help fully understand the importance of physiological effects. The simple model shows that the physiological effect of carbon dioxide is the main driver of future drying over the eastern Amazon. This implies that future changes in rainfall are independent of how much the climate warms. Our findings show the importance of improving understanding of how plants affect atmospheric processes.

1. Introduction

The Amazon rainforest accounts for 40% of global tropical forest area (Aragão et al., 2014) and plays an important role in the global carbon cycle (Malhi et al., 2006). Amazonian vegetation and carbon balance are sensitive to changes in precipitation patterns (Gatti et al., 2014; Hilker et al., 2014; Phillips et al., 2009). However, observed trends and future projections of Amazonian precipitation are highly uncertain (Duffy et al., 2015; Fu et al., 2013; Joetzjer et al., 2013; Orłowski & Seneviratne, 2013).

Observations suggest an increasing trend in drought conditions (Li et al., 2008), and lengthening of the dry season (Fu et al., 2013), but also a stronger wet season (Gloor et al., 2013). Future projections from the Coupled Model Intercomparison Project Phase 5 indicate drying (Boisier et al., 2015), but the intermodel spread is large (Joetzjer et al., 2013). It is difficult to disentangle which drivers are responsible for the projected changes and associated uncertainties. Various factors could influence Amazonian precipitation, including rising temperatures (Boisier et al., 2015; Joetzjer et al., 2013), land use change (Alves et al., 2017; Spracklen & Garcia-Carreras, 2015), and fast responses to atmospheric forcing agents (Andrews, Doutriaux-Boucher,

©2018. The Authors.

This is an open access article under the terms of the Creative Commons Attribution License, which permits use, distribution and reproduction in any medium, provided the original work is properly cited.

et al., 2010; Samset et al., 2016). Fast precipitation responses can occur on time scales of days to weeks due to the near-instantaneous impact on the atmospheric energy budget (Andrews, Forster, et al., 2010; Lambert & Faull, 2007; Mitchell et al., 1987) and can produce significant regional changes (Bony et al., 2013; Richardson et al., 2016; Samset et al., 2016).

CO₂ causes fast precipitation changes not only due to radiative effects but also due to effects on plant stomata (Cao et al., 2009; Andrews, Doutriaux-Boucher, et al., 2010). Higher CO₂ concentrations reduce stomatal opening, decreasing evapotranspiration. This is known as the CO₂ physiological effect (Field et al., 1995; Betts et al., 1997). Around 30% of Amazonian precipitation is thought to be fueled by terrestrial evapotranspiration (Brubaker et al., 1993; Van Der Ent et al., 2010). Given the high level of vegetation and water recycling, the CO₂ physiological effect could strongly affect Amazonian precipitation, as highlighted in previous studies (Abe et al., 2015; Andrews, Doutriaux-Boucher, et al., 2010; Chadwick et al., 2017; Pu & Dickinson, 2014; Skinner et al., 2017). However, the precipitation response is uncertain and poorly understood.

To improve understanding of Amazonian precipitation, we analyze a range of climate simulations from the Precipitation Driver Response Model Intercomparison Project (PDRMIP) and CMIP5, isolating the response to a variety of forcing agents (CO₂, CH₄, SO₄, black carbon (BC), and insolation (SOL)) and examining the role of fast versus slow responses. Using CMIP5 simulations, we isolate the physiological effects of CO₂ on Amazonian precipitation from a multimodel perspective. We construct a simple model for estimating Amazonian precipitation change to establish the main driver of projected changes for the end of the 21st century.

2. Data and Methods

2.1. Precipitation Response to Forcing

Using output from 10 climate models participating in PDRMIP (see Tables S1–S3 in the supporting information and Myhre et al., 2017), we analyze the precipitation response to five abrupt global forcing scenarios: doubling CO₂ concentration (2×CO₂), tripling methane concentration (3×CH₄), 10 times BC concentration or emissions (10×BC), five times sulfate concentration or emissions (5×SO₄), and a 2% increase in insolation (2% SOL). Perturbations are relative to present-day or preindustrial values. Simulations were performed with sea surface temperatures (SSTs) fixed for 15 years and with a coupled ocean for 100 years. Responses are calculated by subtracting a control run from perturbed runs. The PDRMIP models include stomatal conductance sensitivity to CO₂.

We separate the precipitation response into a forcing-dependent fast component and a temperature-driven slow component (Andrews, Forster, et al., 2010). The fast component is taken as the mean response in fixed-SST simulations, in which temperature-driven feedbacks are inhibited. The slow response is calculated using equation (1):

$$\delta P_{\text{slow}} = \delta P_{\text{tot}} - \delta P_{\text{fast}} \quad (1)$$

where δP_{slow} is the slow component, δP_{tot} is the total response (taken as the mean response in the final 50 years of the ocean-coupled simulations), and δP_{fast} is the fast component.

2.2. Energy and Moisture Budget Changes

To understand the precipitation responses, we analyze the local atmospheric energy and moisture budgets that provide constraints on precipitation as shown in equation (2):

$$L\delta P = \delta LWC - \delta SWA - \delta SH + \delta H = \delta LH + L\delta M, \quad (2)$$

where L is the latent heat of condensation, P is local precipitation, LWC is net atmospheric longwave radiative cooling, SWA is net atmospheric shortwave absorption, SH is sensible heat flux from the surface, H is dry static energy (DSE) flux divergence, LH is latent heat flux from the surface, M is moisture convergence, and δ represents a perturbation between climates. δH and δM are calculated as residuals. H is driven by changes in horizontal and vertical winds and DSE gradients. In the tropics horizontal DSE gradients are small; therefore, changes in H are indicative of changes in vertical motions or the vertical temperature profile of the atmosphere (Muller & O’Gorman, 2011).

2.3. CO₂ Physiological Effect

Output from 12 CMIP5 models (Table S5) is used to isolate the CO₂ physiological effect on precipitation. Two sets of experiments (Table S4) are analyzed in which SSTs are fixed, and atmospheric CO₂ quadrupled. One

set includes physiological effects (sstClim and sstClim4×CO₂) and one set does not (amip and amip4×CO₂) (Taylor et al., 2011). The sstClim simulations include a sensitivity of stomatal conductance to CO₂ concentration that determines the evapotranspiration flux (Table S6). In amip simulations either the terrestrial carbon cycle is switched off or vegetation does not see the increase in CO₂.

The response for each set of experiments is calculated by differencing the perturbed run (sstClim4×CO₂ or amip4×CO₂) and respective control run (sstClim or amip). We then isolate the physiological effects by differencing the two sets of experiments. Although baseline SSTs also differ between experiments, the precipitation changes are shown to be driven locally, suggesting SSTs have little effect. Not all models performed both sstClim and amip experiments. Consistent results are obtained when using only models that performed both (Figure S1).

2.4. Projected Precipitation Change

Based on the PDRMIP 2×CO₂ simulations, we construct a simple model to estimate the contribution of CO₂ and increasing temperature to projected Amazonian precipitation change by the end of the 21st century (2081–2100). For each PDRMIP model we compute an *R* factor for CO₂, which is the fast precipitation response per unit global-mean top of the atmosphere (TOA) forcing, and a hydrological sensitivity (HS), which is the slow precipitation response per unit global-mean temperature change, as shown in equations (3) and (4):

$$R = \delta P_{\text{fast}} / F_{\text{CO}_2} \quad (3)$$

$$HS = \delta P_{\text{slow}} / (\delta T_{\text{tot}} - \delta T_{\text{fsst}}) \quad (4)$$

where δP_{fast} and δP_{slow} are the fast and slow precipitation responses to doubling CO₂ (see section 2.1 for fast, slow, and total definitions), F_{CO_2} is global-mean TOA CO₂ forcing, δT_{tot} is the total global-mean surface temperature response, and δT_{fsst} is the global-mean surface temperature response in the fixed-SST simulations (due to land surface). We then use the PDRMIP multimodel mean *R* and HS to estimate precipitation change following two Representative Concentration Pathways, RCP4.5 and RCP8.5, as shown in equation (5):

$$\delta P(t) = (R_{\text{PDRMIP}} \times F_{\text{CO}_2}(t)) + (HS_{\text{PDRMIP}} \times \delta T(t)), \quad (5)$$

where δP is precipitation change at time *t*, R_{PDRMIP} is the PDRMIP multimodel mean *R* factor, F_{CO_2} is global-mean TOA CO₂ forcing at time *t*, HS_{PDRMIP} is the PDRMIP multimodel mean HS, and δT is global-mean surface temperature change at time *t*. F_{CO_2} values are taken from Meinshausen et al. (2011), and δT is taken as the CMIP5 multimodel mean for the years 2081–2100. CMIP5 precipitation and temperature projections are calculated using output from 15 models (Table S5) which include CO₂ physiological effects. Equation (5) is used to estimate precipitation change for the region mean shown in Figure 1a, and spatially by calculating *R* and HS for each grid point.

3. Results and Discussion

3.1. Precipitation Response to Forcing

We first look at the Amazonian precipitation response to individual forcings using the PDRMIP model ensemble (Figure 1). Doubling CO₂ reduces precipitation over much of the Amazon, in particular the central and eastern regions (Figure 1a). Conversely, along the northwestern edge of South America precipitation increases. The models exhibit good agreement on reduced precipitation in the northeast. However, the magnitude of change and how far it extends west is variable.

Increasing BC also drives considerable drying over the Amazon (Figure 1d), with 80% of models agreeing on reductions over much of northern South America. The 3×CH₄, 5×SO₄, and 2%SOL produce only small changes in the central and eastern Amazon (Figures 1b, 1c, and 1e). Sulfate and solar forcing affect precipitation more in the west, with increased insolation enhancing precipitation, and increased sulfate causing drying.

Figure 1f shows the mean precipitation responses for the region outlined in Figure 1a, encompassing eastern and central Amazonia (ECA). The responses are split into contributions from the forcing-dependent fast response, and temperature-driven slow response (temperature responses shown in Figure S2). The ECA region-mean responses to 3×CH₄, 5×SO₄, and 2%SOL are small, though intermodel spread is large. The negligible precipitation response to SO₄ and solar forcing arises due to opposing fast and slow terms. Increased

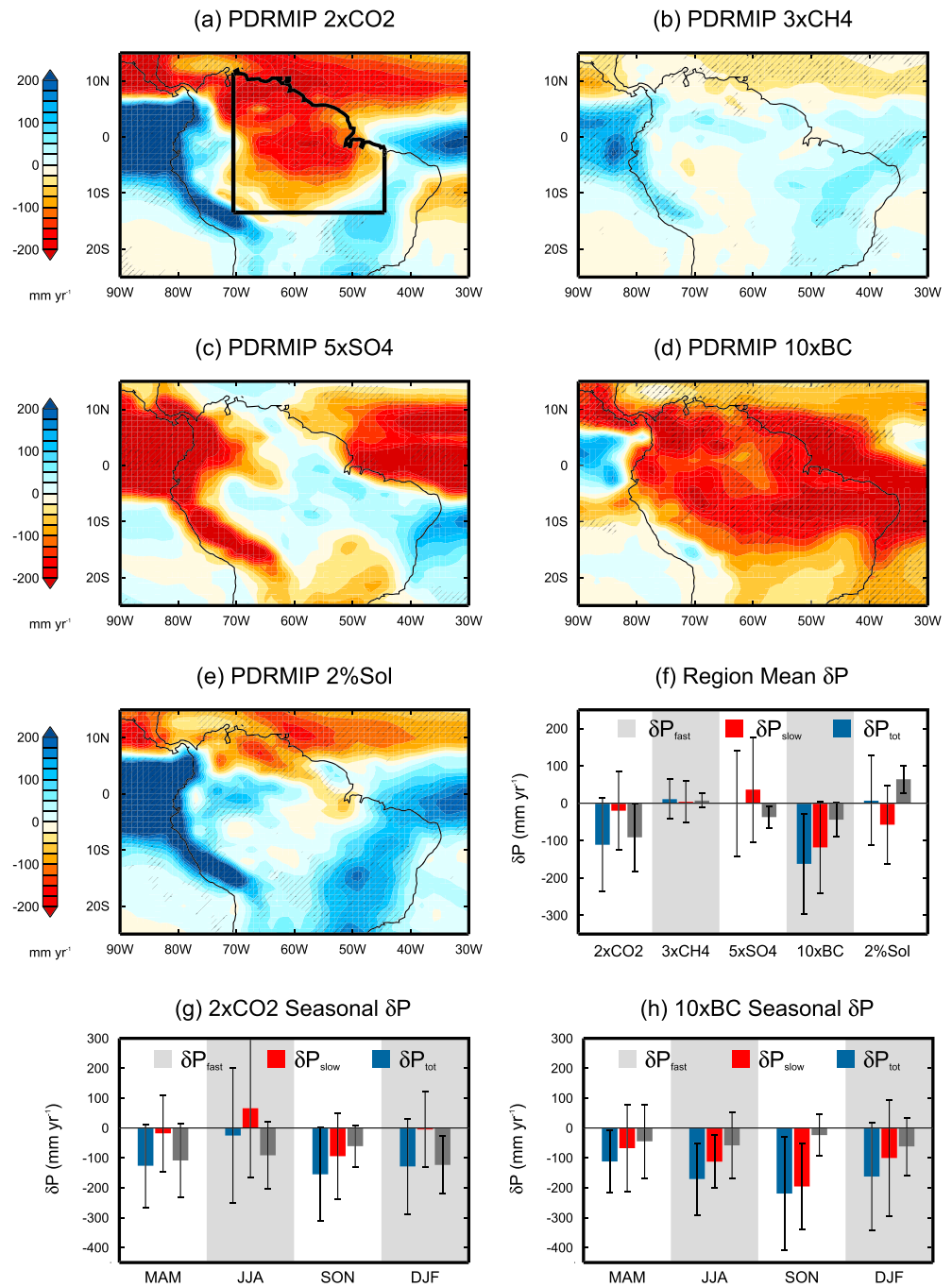


Figure 1. Precipitation Driver Response Model Intercomparison Project (PDRMIP) multimodel mean total precipitation response to (a) $2\times\text{CO}_2$, (b) $3\times\text{CH}_4$, (c) $5\times\text{SO}_4$, (d) $10\times\text{BC}$, and (e) $2\%\text{SOL}$. Hatching denotes where 80% of models agree on sign of change. Panel (f) shows the PDRMIP multimodel mean precipitation response for the eastern and central Amazonia region outlined in panel (a). Total response shown in blue, fast component in gray, and slow component in red. Panels (g) and (h) show the seasonal response to $2\times\text{CO}_2$ and $10\times\text{BC}$. Error bars denote model spread standard deviation.

SO_4 produces a negative fast response, mainly due to reduced DSE flux divergence (Figure S3a). This can be explained by reduced downwelling shortwave radiation at the surface, which reduces the land-sea temperature contrast, reducing convection and precipitation over land (Chadwick et al., 2014; Richardson et al., 2016). The opposite effect occurs for solar forcing. The slow response counteracts these changes; increasing precipitation as global temperatures decrease due to SO_4 , and decreasing precipitation as the

climate warms due to solar forcing. The model-mean slow response is negative per unit temperature change for all scenarios except $3\times\text{CH}_4$, but the magnitude varies (Figure S3b).

Increased CO_2 drives a large reduction in precipitation over the ECA region. The response is dominated by the fast component ($-91.1 \pm 90.6 \text{ mm yr}^{-1}$), compared to the slow ($-19.9 \pm 104.4 \text{ mm yr}^{-1}$). Despite considerable model spread, the negative fast response is very consistent, with 90% of models agreeing on sign. Although the fast component dominates the model mean, the slow component often contributes significantly in individual models. In 50% of models the temperature-driven responses are larger than the fast component, but there is little agreement on sign.

Increased BC drives reduced precipitation over the ECA region. The model-mean response to $10\times\text{BC}$ is dominated by the temperature-driven response ($-118.3 \pm 122.3 \text{ mm yr}^{-1}$), rather than the fast component ($-44.0 \pm 45.3 \text{ mm yr}^{-1}$). The intermodel spread is large, but the sign of change is robust across models.

Figure 1g shows the seasonal breakdown of the ECA region-mean $2\times\text{CO}_2$ precipitation response. The slow response causes reduced SON precipitation, indicating a strengthening of the late dry season. Previous studies have shown that future projections suggest a strengthened and longer dry season (Boisier et al., 2015; Joetzjer et al., 2013). However, the slow response also enhances JJA precipitation, resulting in little annual-mean change. The fast response drives reduced precipitation throughout the year, with the largest reduction during the wet season.

BC drives larger reductions in precipitation during the dry season (Figure 1h), when higher levels of biomass burning occur in South America. Hodnebrog et al. (2016) similarly found that BC most strongly affects precipitation in South Africa during the dry season.

3.2. Energy and Moisture Budget Changes

To understand the mechanisms driving the ECA region-mean precipitation response to CO_2 and BC, we analyze the energy and moisture budgets (Figure 2). The negative CO_2 fast response arises mainly due to repartitioning of sensible and latent heat fluxes, as well as reduced LW cooling (Figure 2a). CO_2 strongly affects surface heat fluxes, reducing LH and increasing SH. The changes in surface fluxes are caused by physiological effects (see section 3.3). The changes in horizontal heat and moisture transport, associated with circulation, are very uncertain. The LH response also exhibits considerable intermodel spread and is highly correlated with the fast precipitation response intermodel spread ($r = 0.92$). Given that both evapotranspiration and precipitation decrease, the change in surface runoff ($P - E$, equivalent to M) is relatively small ($-21.8 \pm 51.1 \text{ mm yr}^{-1}$).

The negative fast precipitation response to BC is driven by increased atmospheric shortwave absorption (Figure 2c). The uncertainty largely arises from the circulation response, with changes in moisture convergence contributing strongly to intermodel spread ($r^2 = 0.90$).

The slow response to $2\times\text{CO}_2$ is small due to counteracting energy budget feedbacks (Figure 2b). LW cooling increases with warming, which is countered by increased SW absorption, increased SH, and reduced divergence of DSE flux. The LW and SW radiative feedbacks per unit Kelvin are fairly consistent across forcing scenarios (Figure S3). The different slow precipitation responses across forcings largely arise from the SH feedbacks.

For $2\times\text{CO}_2$, changes in horizontal DSE and moisture fluxes are very uncertain (Figure 2b) and contribute strongly to intermodel spread in the slow precipitation response ($r^2 = 0.92$ and $r^2 = 0.85$). Therefore, although the model-mean slow response is small, in individual models temperature-driven circulation changes can drive large changes in precipitation. However, the slow response shows little agreement in sign or magnitude. Circulation changes are known to be important for tropical precipitation patterns (Chadwick et al., 2013; Chou et al., 2009; Seager et al., 2010). Future circulation changes are uncertain and may be strongly influenced by chaotic natural variability and model errors (Shepherd, 2014).

Despite causing a weak global temperature response, $10\times\text{BC}$ produces a large negative slow precipitation response over the Amazon. The slow response is robustly negative but variable in magnitude. This is mainly driven by circulation changes, indicated by reduced divergence of DSE flux and moisture convergence (Figure 2d). BC has been shown to drive northward shifts in the intertropical convergence zone (ITCZ) in

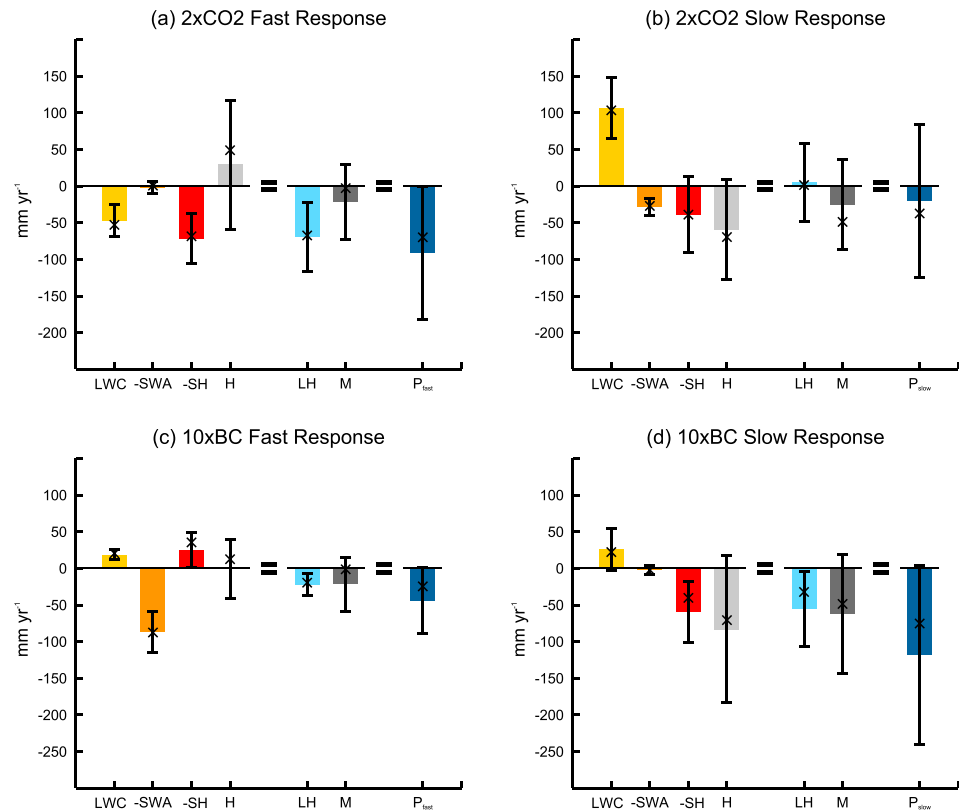


Figure 2. Precipitation Driver Response Model Intercomparison Project multimodel mean precipitation, energy, and moisture budget (see equation (2)) responses to (a, b) $2\times\text{CO}_2$ and (c, d) $10\times\text{BC}$, split into (a, c) fast and (b, d) slow components, for the eastern and central Amazonia region. Signs for terms are given according to equation (2). Crosses indicate the median and error bars denote model spread standard deviation.

models (Chung & Seinfeld, 2005; Jones et al., 2007; Kovilakam & Mahajan, 2015), due to the forcing asymmetry. The ITCZ shift is evident in the slow precipitation response spatial pattern (Figure S4). These circulation changes, combined with a repartitioning of LH and SH, drive the negative slow precipitation response. However, it should be noted that the $10\times\text{BC}$ perturbation is large. If the total precipitation response is linearly scaled based on TOA forcing to present-day levels (1981–2000) relative to preindustrial, the response reduces to $-25.9 \pm 8.3 \text{ mm yr}^{-1}$.

The largest increases in BC occur over Asia (Myhre et al., 2017). However, the large changes in BC over Asia drive very little change in Amazonian precipitation (Figure S5), indicating local biomass burning emissions drive the response.

3.3. CO_2 Physiological Effect

Figure 3 shows the role of physiological effects on plants in driving the fast precipitation response to CO_2 by comparing CMIP5 sstClim4 $\times\text{CO}_2$ simulations (include physiological effects) and amip4 $\times\text{CO}_2$ simulations (do not include physiological effects). In the amip4 $\times\text{CO}_2$ simulations multimodel mean precipitation increases over most of tropical South America. In contrast, in the sstClim4 $\times\text{CO}_2$ simulations drying extends much further inland from the east. Figure 3c shows the difference between scenarios. Over much of the Amazon, particularly in the east, CO_2 physiological effects drive considerable drying. In contrast, along the west coast precipitation is enhanced. The multimodel mean response is generally in agreement with previous single-model studies (Abe et al., 2015; Andrews, Doutriaux-Boucher, et al., 2010; Pu & Dickinson, 2014; Skinner et al., 2017).

Figure 3d shows the physiological effects on energy and moisture budgets for the ECA region. The reduced precipitation due to CO_2 physiological forcing is almost entirely due to repartitioning of sensible and latent

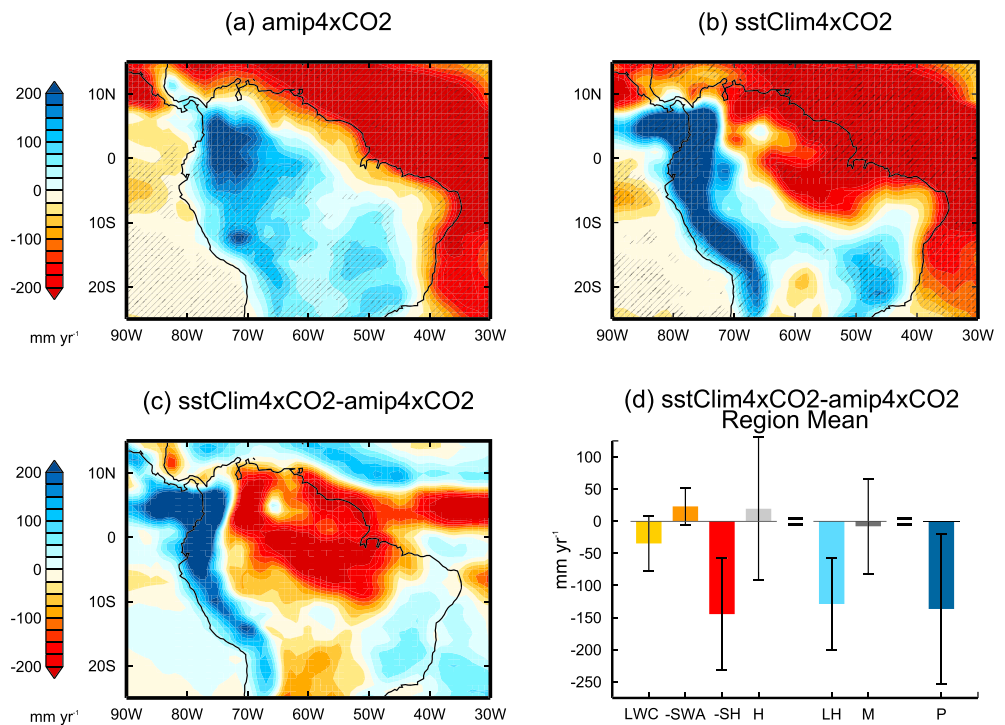


Figure 3. Coupled Model Intercomparison Project Phase 5 multimodel mean precipitation response to quadrupling CO_2 in (a) amip and (b) sstClim simulations and (c) the difference. Hatching shows where 80% of models agree on sign of change (not applicable in panel (c)). Panel d shows the difference between sstClim and amip energy and moisture budget responses for the eastern and central Amazonia region. Error bars denote the model spread standard deviation.

heat fluxes. Increased CO_2 reduces stomatal conductance (Field et al., 1995), reducing evapotranspiration. In the Amazon, where water recycling is important (Zemp et al., 2014), the reduction in evapotranspiration drives considerable drying. Surface energy balance is maintained through increased SH flux. There is very little change in horizontal heat and moisture fluxes, indicating the importance of local changes.

The strongest reductions in precipitation occur in the eastern and central Amazon. This may be because the evaporation recycling ratio (fraction of local evaporation which returns as local precipitation) is higher in the east (Van Der Ent et al., 2010). The increase in precipitation along the west coast is consistent with Skinner et al. (2017), who found that decreased evapotranspiration warms the land surface and draws moisture from the nearby ocean, increasing convective instability and heavy rainfall events.

The CO_2 physiological effect also drives a large fraction of the fast precipitation response uncertainty for the ECA region. The intermodel standard deviation in the sstClim4x CO_2 simulations (109 mm yr^{-1}) is over double that for amip4x CO_2 (42 mm yr^{-1}). Including CO_2 physiological effects considerably increases the uncertainty in latent and sensible heat flux responses (Figure S6), which contribute strongly to the large model spread. In addition, the uncertain response of surface heat fluxes leads to more uncertainty in the horizontal transport of energy and moisture. This is consistent with studies which have shown uncertainty in transpiration sensitivity contributes strongly to uncertainty in the global-mean fast precipitation response to CO_2 (DeAngelis et al., 2016) and future projections of terrestrial precipitation (Mengis et al., 2015).

3.4. Projected Precipitation Change

We have shown that the reduction in precipitation over central and eastern Amazonia in response to CO_2 is dominated by the fast component, which is driven by physiological effects on evapotranspiration. Therefore, given that CO_2 forcing increasingly dominates in future emission scenarios (van Vuuren et al., 2011), the CO_2 physiological effect could play a key role in projections. To quantify the potential contribution of CO_2 to precipitation change over the Amazon by the end of the 21st century, we construct a simple model based on the PDRMIP results. Precipitation change over the Amazon is estimated by scaling the fast component based on

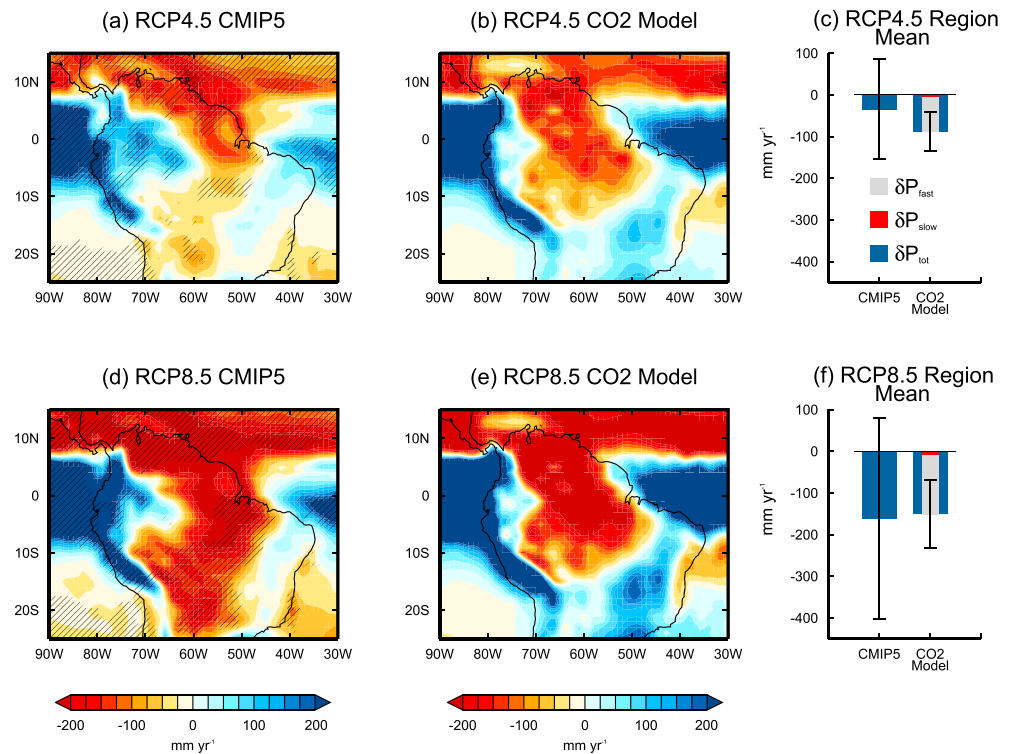


Figure 4. Projected precipitation change for 2081–2100 relative to preindustrial, following (a–c) Representative Concentration Pathways (RCP) 4.5 and (d–f) RCP8.5, calculated using (a, d) Coupled Model Intercomparison Project Phase 5 multimodel mean (only models which include CO₂ physiological effects) and (b, e) the simple model given by equation (5). Hatching denotes where 80% of models agree on sign of change. Panels (c) and (f) show mean change for the eastern and central Amazonia region. Total change in blue, the fast component in gray, and slow component in red. Error bars denote the standard deviation of CMIP5 model spread, and the standard error of the simple model.

CO₂ TOA forcing for the end of the century and scaling the slow component based on global-mean surface temperature change (equation (5)). The simple model is compared with CMIP5 multimodel mean projections, calculated using 15 models (Table S5) which include physiological effects (Collins et al., 2013), in Figure 4.

The CMIP5 projections indicate drying over large areas of the Amazon particularly in the east, south, and north. In contrast, along the west coast of South America precipitation increases. Changes are larger for RCP8.5, following a business as usual emissions scenario, but the spatial pattern is very similar. Despite the large predicted changes, there is considerable variation across models. Over tropical South America there are very few regions in which more than 80% of models agree on the sign of change. Although agreement on the spatial pattern is low, models consistently project large changes (Chadwick et al., 2015).

The simple model predicts a similar drying ($-151.1 \pm 82 \text{ mm yr}^{-1}$) over the ECA region as CMIP5 projections ($-160.9 \pm 241 \text{ mm yr}^{-1}$) following RCP8.5, driven almost entirely by the fast response to CO₂. For RCP4.5 the simple model predicts more drying ($-87.1 \pm 47 \text{ mm yr}^{-1}$) than CMIP5 projections ($-34.5 \pm 120 \text{ mm yr}^{-1}$). The comparison suggests that projected drying in the ECA region is predominantly driven by CO₂ physiological forcing. Therefore, projected drying is independent of increasing temperatures, as supported by the lack of correlation between global-mean warming and precipitation change across CMIP5 models ($r = 0.16$ and -0.09 for RCP4.5 and RCP8.5).

Spatially, there are very similar features between the simple model and CMIP5 projections. These include significant drying over the eastern, southern, and northern Amazon, and increased precipitation in the west, all of which are predominantly driven by the fast response to CO₂ (Figure S7). There are some notable differences, such as in the western Amazon, where enhanced precipitation extends further east in CMIP5 projections. This may be due to drivers not included in the simple model, such as land use change, aerosols, and

greenhouse gases other than CO₂. Land use change is likely to be the most influential forcing not included (Spracklen & Garcia-Carreras, 2015) and may account for the difference between the simple model and CMIP5 projections for the ECA region-mean under RCP4.5.

The simple model indicates that CO₂ physiological forcing could dominate multimodel mean future projections of precipitation change over large areas of the Amazon. However, individual models show that temperature-driven circulation changes can be large but are highly uncertain and show little agreement.

4. Conclusions

We have presented the Amazonian precipitation response to individual atmospheric forcings using the PDRMIP model ensemble. Precipitation changes exhibit considerable intermodel spread, but there are some robust signals. Increased BC drives a robust drying over the Amazon; however, the magnitude of change varies across models. The reduction in precipitation is largely due to temperature-driven circulation changes, associated with a northward shift in the ITCZ. The fast precipitation response to BC also contributes to drying due to enhanced SW absorption.

Increased CO₂ concentrations drive reduced Amazonian precipitation, particularly in the east. The model-mean drying is dominated by the fast component, for which 90% of models agree on reduced precipitation over the ECA region. Using CMIP5 model output, we find that physiological effects dominate the fast response to CO₂ over the Amazon, through a change in partitioning of sensible and latent heat fluxes. Higher CO₂ concentrations reduce stomatal opening and consequently evapotranspiration. This limits moisture availability and precipitation over much of the Amazon, particularly in the east. Physiological effects also drive increased precipitation along the west coast. Physiological effects contribute strongly to the uncertainty in Amazonian precipitation changes, over doubling the intermodel spread for the ECA region.

Using a simple model based on CO₂ TOA forcing and global-mean surface temperature change, we quantify the potential contribution of CO₂ to precipitation changes over the Amazon by the end of the century (2081–2100) relative to preindustrial. The simple model suggests that CMIP5 multimodel mean projected drying over the ECA region is predominantly driven by CO₂ physiological effects. This implies that projected Amazonian precipitation change is independent of rising temperatures, being mainly driven by atmospheric CO₂ concentration. However, it should be noted that temperature-driven changes can be large in individual models but show little agreement. Our findings illustrate the importance of short-time scale processes on long-term precipitation change in this region and highlight the need to reduce uncertainties associated with vegetation schemes.

References

- Abe, M., Shiogama, H., Yokohata, T., Emori, S., & Nozawa, T. (2015). Asymmetric impact of the physiological effect of carbon dioxide on hydrological responses to instantaneous negative and positive CO₂ forcing. *Climate Dynamics*, *45*(7–8), 2181–2192. <https://doi.org/10.1007/s00382-014-2465-1>
- Alves, L. M., Marengo, J. A., Fu, R., & Bombardi, R. J. (2017). Sensitivity of Amazon regional climate to deforestation. *American Journal of Climate Change*, *06*(01), 75–98. <https://doi.org/10.4236/ajcc.2017.61005>
- Andrews, T., Doutriaux-Boucher, M., Boucher, O., & Forster, P. M. (2010). A regional and global analysis of carbon dioxide physiological forcing and its impact on climate. *Climate Dynamics*, *36*(3–4), 783–792. <https://doi.org/10.1007/s00382-010-0742-1>
- Andrews, T., Forster, P. M., Boucher, O., Bellouin, N., & Jones, A. (2010). Precipitation, radiative forcing and global temperature change. *Geophysical Research Letters*, *37*, L14701. <https://doi.org/10.1029/2010GL043991>
- Aragão, L. E. O. C., Poulter, B., Barlow, J. B., Anderson, L. O., Malhi, Y., Saatchi, S., et al. (2014). Environmental change and the carbon balance of Amazonian forests. *Biological Reviews*, *89*(4), 913–931. <https://doi.org/10.1111/brv.12088>
- Betts, A. R., Cox, P. M., & Lee, S. E. (1997). Contrasting physiological and structural vegetation feedbacks in climate change simulations. *Nature*, *387*(6635), 796–799. <https://doi.org/10.1038/42924>
- Boisier, J. P., Ciais, P., Ducharne, A., & Guimberteau, M. (2015). Projected strengthening of Amazonian dry season by constrained climate model simulations. *Nature Climate Change*, *5*(7), 656–660. <https://doi.org/10.1038/nclimate2658>
- Bony, S., Bellon, G., Klocke, D., Sherwood, S., Fermepein, S., & Denvil, S. (2013). Robust direct effect of carbon dioxide on tropical circulation and regional precipitation. *Nature Geoscience*, *6*(6), 447–451. <https://doi.org/10.1038/ngeo1799>
- Brubaker, K. L., Entekhabi, D., & Eagleson, P. S. (1993). Estimation of continental precipitation recycling. *Journal of Climate*, *6*(6), 1077–1089. [https://doi.org/10.1175/1520-0442\(1993\)006%3C1077:EOCPR%3E2.0.CO;2](https://doi.org/10.1175/1520-0442(1993)006%3C1077:EOCPR%3E2.0.CO;2)
- Cao, L., Bala, G., Caldeira, K., Nemani, R., & Ban-Weiss, G. (2009). Climate response to physiological forcing of carbon dioxide simulated by the coupled Community Atmosphere Model (CAM3.1) and Community Land Model (CLM3.0). *Geophysical Research Letters*, *36*, L10402. <https://doi.org/10.1029/2009GL037724>
- Chadwick, R., Boutle, I., & Martin, G. (2013). Spatial patterns of precipitation change in CMIP5: Why the rich do not get richer in the tropics. *Journal of Climate*, *26*(11), 3803–3822. <https://doi.org/10.1175/JCLI-D-12-00543.1>

Acknowledgments

CMIP5 and PDRMIP model output is publicly available for download (see <http://pcmdi9.llnl.gov> and <http://www.cicero.uio.no/en/PDRMIP/PDRMIP-data-access>, respectively). T. B. R. was supported by a NERC CASE award in collaboration with the Met Office NE/K007483/1 and NERC grant NE/N006038/1. P. M. F. was supported by a Royal Society Wolfson Merit Award and NERC grant NE/N006038/1. T. A. was supported by the Newton Fund through the Met Office Climate Science for Service Partnership Brazil (CSSP Brazil). B. H. S. and G. M. were funded by the Research Council of Norway, through the grant NAPEX (229778). D. S. and G. F. thank NASA GISS for funding and acknowledge the NASA High-End Computing Program through the NASA Center for Climate Simulation at Goddard Space Flight Center for computational resources. O. B. acknowledges HPC resources from TGCC under the gencmip6 allocation provided by GENCI (Grand Equipement National de Calcul Intensif). T. T. is supported by the NEC SX-ACE supercomputer system of the National Institute for Environmental Studies, Japan, the Environmental Research and Technology Development Fund (S-12-3) of the Ministry of Environment, Japan, and JSPS KAKENHI grant JP15H01728 and JP15K12190. M. K., D. S., and A. V. were supported by the Natural Environment Research Council under grant NE/K500872/1 and from the Grantham Institute at Imperial College. Simulations with HadGEM2 and HadGEM3-GA4 were performed using the MONSoon system, a collaborative facility supplied under the Joint Weather and Climate Research Programme, which is a strategic partnership between the Met Office and the Natural Environment Research Council. D. O. and A. K. were supported by the Norwegian Research Council through the projects EVA (grant 229771), EarthClim (207711/E10), NOTUR (nn2345k), and NorStore (ns2345k).

- Chadwick, R., Douville, H., & Skinner, C. B. (2017). Timeslice experiments for understanding regional climate projections: Applications to the tropical hydrological cycle and European winter circulation. *Climate Dynamics*, *49*(9-10), 3011–3029. <https://doi.org/10.1007/s00382-016-3488-6>
- Chadwick, R., Good, P., Andrews, T., & Martin, G. (2014). Surface warming patterns drive tropical rainfall pattern responses to CO₂ forcing on all timescales. *Geophysical Research Letters*, *41*, 610–615. <https://doi.org/10.1002/2013GL058504>
- Chadwick, R., Good, P., Martin, G., & Rowell, D. P. (2015). Large rainfall changes consistently projected over substantial areas of tropical land. *Nature Climate Change*, *6*(2), 177–181. <https://doi.org/10.1038/nclimate2805>
- Chou, C., Neelin, J. D., Chen, C.-A., & Tu, J.-Y. (2009). Evaluating the “rich-get-richer” mechanism in tropical precipitation change under global warming. *Journal of Climate*, *22*(8), 1982–2005. <https://doi.org/10.1175/2008JCLI2471.1>
- Chung, S., & Seinfeld, J. (2005). Climate response of direct radiative forcing of anthropogenic black carbon. *Journal of Geophysical Research*, *110*, D11102. <https://doi.org/10.1029/2004JD005441>
- Collins, M., Knutti, R., Arblaster, J., Dufresne, J.-L., Fichefet, T., Friedlingstein, P., et al. (2013). Long-term climate change: Projections, commitments and irreversibility. In *Climate Change 2013: The Physical Science Basis. Contribution of Working Group I to the Fifth Assessment Report of the Intergovernmental Panel on Climate Change* (pp. 1029–1136). <https://doi.org/10.1017/CBO9781107415324.024>
- DeAngelis, A. M., Qu, X., & Hall, A. (2016). Importance of vegetation processes for model spread in the fast precipitation response to CO₂ forcing. *Geophysical Research Letters*, *43*, 12,550–12,559. <https://doi.org/10.1002/2016GL071392>
- Duffy, P. B., Brando, P., Asner, G. P., & Field, C. B. (2015). Projections of future meteorological drought and wet periods in the Amazon. *Proceedings of the National Academy of Sciences*, *112*(43), 13,172–13,177. <https://doi.org/10.1073/pnas.1421010112>
- Field, C. B., Jackson, R. B., & Mooney, H. A. (1995). Stomatal responses to increased CO₂: Implications from the plant to the global scale. *Plant, Cell and Environment*, *18*(10), 1214–1225. <https://doi.org/10.1111/j.1365-3040.1995.tb00630.x>
- Fu, R., Yin, L., Li, W., Arias, P. A., Dickinson, R. E., Huang, L., et al. (2013). Increased dry-season length over southern Amazonia in recent decades and its implication for future climate projection. *Proceedings of the National Academy of Sciences*, *110*(45), 18,110–18,115. <https://doi.org/10.1073/pnas.1302584110>
- Gatti, L. V. (2014). Drought sensitivity of Amazonian carbon balance revealed by atmospheric measurements. *Nature*, *506*(7486), 76–80. <https://doi.org/10.1038/nature12957>
- Gloor, M., Brienen, R. J. W., Galbraith, D., Feldpausch, T. R., Schöngart, J., Guyot, J. L., et al. (2013). Intensification of the Amazon hydrological cycle over the last two decades. *Geophysical Research Letters*, *40*, 1729–1733. <https://doi.org/10.1002/grl.50377>
- Hilker, T., Lyapustin, A. I., Tucker, C. J., Hall, F. G., Myneni, R. B., Wang, Y., et al. (2014). Vegetation dynamics and rainfall sensitivity of the Amazon. *Proceedings of the National Academy of Sciences*, *111*(45), 16,041–16,046. <https://doi.org/10.1073/pnas.1404870111>
- Hodnebrog, Ø., Myhre, G., Forster, P. M., Sillmann, J., & Samset, B. H. (2016). Local biomass burning is a dominant cause of the observed precipitation reduction in southern Africa. *Nature Communications*, *7*, 11236. <https://doi.org/10.1038/ncomms11236>
- Joetzer, E., Douville, H., Delire, C., & Ciais, P. (2013). Present-day and future Amazonian precipitation in global climate models: CMIP5 versus CMIP3. *Climate Dynamics*, *41*(11–12), 2921–2936. <https://doi.org/10.1007/s00382-012-1644-1>
- Jones, A., Haywood, J. M., & Boucher, O. (2007). Aerosol forcing, climate response and climate sensitivity in the Hadley Centre climate model. *Journal of Geophysical Research*, *112*, D20211. <https://doi.org/10.1029/2007JD008688>
- Kovilakam, M., & Mahajan, S. (2015). Black carbon aerosol-induced Northern Hemisphere tropical expansion. *Geophysical Research Letters*, *42*, 4964–4972. <https://doi.org/10.1002/2015GL064559>
- Lambert, F. H., & Faull, N. E. (2007). Tropospheric adjustment: The response of two general circulation models to a change in insolation. *Geophysical Research Letters*, *34*, L03701. <https://doi.org/10.1029/2006GL028124>
- Li, W., Fu, R., Juárez, R. I. N., & Fernandes, K. (2008). Observed change of the standardized precipitation index, its potential cause and implications to future climate change in the Amazon region. *Philosophical Transactions of the Royal Society of London. Series B, Biological Sciences*, *363*(1498), 1767–1772. <https://doi.org/10.1098/rstb.2007.0022>
- Malhi, Y., Wood, D., Baker, T. R., Wright, J., Phillips, O. L., Cochrane, T., et al. (2006). The regional variation of aboveground live biomass in old-growth Amazonian forests. *Global Change Biology*, *12*(7), 1107–1138. <https://doi.org/10.1111/j.1365-2486.2006.01120.x>
- Meinshausen, M., Smith, S. J., Calvin, K., Daniel, J. S., Kainuma, M. L. T., Lamarque, J. F., et al. (2011). The RCP greenhouse gas concentrations and their extensions from 1765 to 2300. *Climatic Change*, *109*(1-2), 213–241. <https://doi.org/10.1007/s10584-011-0156-z>
- Mengis, N., Keller, D. P., Eby, M., & Oschlies, A. (2015). Uncertainty in the response of transpiration to CO₂ and implications for climate change. *Environmental Research Letters*, *10*(9), 94001. <https://doi.org/10.1088/1748-9326/10/9/094001>
- Mitchell, J., Wilson, C., & Cunningham, W. (1987). On CO₂ climate sensitivity and model dependence of results. *Quarterly Journal of the Royal Meteorological Society*, *113*(475), 293–322. <https://doi.org/10.1256/smsqj.47516>
- Muller, C. J., & O’Gorman, P. a. (2011). An energetic perspective on the regional response of precipitation to climate change. *Nature Climate Change*, *1*(5), 266–271. <https://doi.org/10.1038/nclimate1169>
- Myhre, G., Forster, P. M., Samset, B. H., Hodnebrog, Ø., Sillmann, J., Aalbergjø, S. G., et al. (2017). PDRMIP: A precipitation driver and response model intercomparison project—Protocol and preliminary results. *Bulletin of the American Meteorological Society*, *98*(6), 1185–1198. <https://doi.org/10.1175/BAMS-D-16-0019.1>
- Orlowsky, B., & Seneviratne, S. I. (2013). Elusive drought: Uncertainty in observed trends and short-and long-term CMIP5 projections. *Hydrology and Earth System Sciences*, *17*(5), 1765–1781. <https://doi.org/10.5194/hess-17-1765-2013>
- Phillips, O. L., Aragão, L. E. O. C., Lewis, S. L., Fisher, J. B., Lloyd, J., López-González, G., et al. (2009). Drought sensitivity of the Amazon rainforest. *Science*, *323*(5919), 1344–1347. <https://doi.org/10.1126/science.1164033>
- Pu, B., & Dickinson, R. E. (2014). Hydrological changes in the climate system from leaf responses to increasing CO₂. *Climate Dynamics*, *42*(7–8), 1905–1923. <https://doi.org/10.1007/s00382-013-1781-1>
- Richardson, T. B., Forster, P. M., Andrews, T., & Parker, D. J. (2016). Understanding the rapid precipitation response to CO₂ and aerosol forcing on a regional scale*. *Journal of Climate*, *29*(2), 583–594. <https://doi.org/10.1175/JCLI-D-15-0174.1>
- Samset, B. H., Myhre, G., Forster, P. M., Hodnebrog, Ø., Andrews, T., Faluvegi, G., et al. (2016). Fast and slow precipitation responses to individual climate forcings: A PDRMIP multimodel study. *Geophysical Research Letters*, *43*, 2782–2791. <https://doi.org/10.1002/2016GL068064>
- Seager, R., Naik, N., & Vecchi, G. A. (2010). Thermodynamic and dynamic mechanisms for large-scale changes in the hydrological cycle in response to global warming. *Journal of Climate*, *23*(17), 4651–4668. <https://doi.org/10.1175/2010JCLI3655.1>
- Shepherd, T. G. (2014). Atmospheric circulation as a source of uncertainty in climate change projections. *Nature Geoscience*, *7*(10), 703–708. <https://doi.org/10.1038/ngeo2253>
- Skinner, C. B., Poulsen, C. J., Chadwick, R., Diffenbaugh, N. S., & Fiorella, R. P. (2017). The role of plant CO₂ physiological forcing in shaping future daily-scale precipitation. *Journal of Climate*, *30*(7), 2319–2340. <https://doi.org/10.1175/JCLI-D-16-0603.1>

- Spracklen, D. V., & Garcia-Carreras, L. (2015). The impact of Amazonian deforestation on Amazon basin rainfall. *Geophysical Research Letters*, 42, 9546–9552. <https://doi.org/10.1002/2015GL066063>
- Taylor, K. E., Stouffer, R. J., & Meehl, G. A. (2011). A summary of the CMIP5 experiment design, 4(January 2011), 1–33.
- Van Der Ent, R. J., Savenije, H. H. G., Schaeffli, B., & Steele-Dunne, S. C. (2010). Origin and fate of atmospheric moisture over continents. *Water Resources Research*, 46, W09525. <https://doi.org/10.1029/2010WR009127>
- van Vuuren, D. P., Edmonds, J., Kainuma, M., Riahi, K., Thomson, A., Hibbard, K., et al. (2011). The representative concentration pathways: An overview. *Climatic Change*, 109(1-2), 5–31. <https://doi.org/10.1007/s10584-011-0148-z>
- Zemp, D. C., Schleussner, C. F., Barbosa, H. M. J., Van Der Ent, R. J., Donges, J. F., Heinke, J., et al. (2014). On the importance of cascading moisture recycling in South America. *Atmospheric Chemistry and Physics*, 14(23), 13,337–13,359. <https://doi.org/10.5194/acp-14-13337-2014>